J|A|C|S
ARTICLES
Published on Web 04/12/2006

Evidence for Two Ferryl Species in Chloroperoxidase Compound II

Kari L. Stone,[†] Lee M. Hoffart,[‡] Rachel K. Behan,[†] Carsten Krebs,[†,‡] and Michael T. Green*,[†]

Contribution from the Departments of Chemistry and Biochemistry and Molecular Biology, The Pennsylvania State University, University Park, Pennsylvania 16802

Received November 20, 2005; E-mail: mtg10@psu.edu

Abstract: Using a combination of density functional calculations and Mössbauer spectroscopy, we have examined chloroperoxidase compound II (CPO-II). The Mössbauer spectrum of CPO-II suggests the presence of two distinct ferryl species in an ~70:30 ratio. Density functional calculations and cryogenic reduction and annealing experiments allow us to assign the major species as an Fe(IV)OH intermediate. The Mössbauer parameters of the minor component are indicative of an authentic iron(IV)oxo species, but we have found the 70:30 ratio to be pH invariant. The unchanging ratio of component concentrations is in agreement with CPO-II's visible absorption spectrum, which shows no change over the enzyme's range of pH stability.

Introduction

Cytochromes P450 are thiolate-ligated heme enzymes that play critical roles in xenobiotic metabolism, neurological development, blood pressure control, and immune defense.[1−5] Interest in these systems stems not only from their biological importance but also from a desire to harness their synthetic potential. P450s are unique among oxidative heme enzymes in that they catalyze the insertion of an oxygen atom, derived either from peroxide or molecular oxygen, into a variety of organic substrates, often with high degrees of regio- and stereoselectivity.[6]

A recent report has suggested a novel role for thiolate ligation in these enzymes. X-ray absorption measurements on the thiolate-ligated iron(IV)oxo (ferryl) in chloroperoxidase compound II (CPO-II) indicate an Fe−O bond of 1.82 Å for this intermediate (pH 6.5).[7] This value is longer than expected for an authentic ferryl unit (typically near 1.65 Å) but in excellent agreement with density functional calculations on a protonated ferryl heme (Fe(IV)−OH, 1.81 Å). The existence of a basic ferryl species has important implications for P450 chemistry.

In the consensus P450 hydroxylation mechanism, a ferryl-radical species called compound I abstracts hydrogen from substrate to form a protonated ferryl (similar to CPO-II), which subsequently hydroxylates the substrate radical (Figure 1). The ability of metal-oxos to abstract hydrogen has been shown to scale with the strength of the O−H bond formed during hydrogen atom abstraction, D(O−H).[8] This energy is determined by the reduction potential of compound I and the pK_a of compound II, as in eq 1.[8,9]

$$\mathrm{D(O{-}H)} = -23.06 \times E^{0}_{\mathrm{cmpd-I}} - 1.37 \times \mathrm{p}K_{\mathrm{a\ cmpd-II}} - 57 \pm 2\ \mathrm{(kcal/mol)} \quad (1)$$

Equation 1 highlights the importance of the ferryl pK_a and suggests that Nature may be using basic thiolate-ligated ferryls to promote hydrogen abstraction (and subsequent hydroxylation) at biologically viable compound I reduction potentials.[7]

This theory rests upon two important assumptions: (1) that the rebound mechanism is operative in P450 hydroxylations, and (2) that basic ferryls are a general and unique feature of thiolate-ligated hemes. The first of these assumptions appears well founded, as experimental and theoretical investigations continue to support the rebound mechanism.[10,11] The merit of the second assumption is not as clear.

Recent crystallographic reports have suggested that other (nonthiolate-ligated) ferryl species may be protonated as well. The Fe−O bond lengths in HRP-II (pH 6.5), myoglobin-II (Mb-II, pH 5.2), cytochrome *c* peroxidase-I (CCP-I, pH 6), and catalase-II (CAT-II, pH 5.2) have been reported to be 1.84, 1.92, 1.87, and 1.87 Å, respectively.[12−15]

[†] Department of Chemistry.
[‡] Department of Biochemistry and Molecular Biology.

(1) Daborn, P. J.; Yen, J. L.; Bogwitz, M. R.; Le Goff, G.; Feil, E.; Jeffers, S.; Tijet, N.; Perry, T.; Heckel, D.; Batterham, P.; Feyereisen, R.; Wilson, T. G.; ffrench-Constant, R. H. *Science* **2002**, *297*, 2253−2256.
(2) Nelson, R. J.; Demas, G. E.; Huang, P. L.; Fishman, M. C.; Dawson, V. L.; Dawson, T. M.; Snyder, S. H. *Nature* **1995**, *378*, 383−386.
(3) Huang, P. L.; Huang, Z. H.; Mashimo, H.; Bloch, K. D.; Moskowitz, M. A.; Bevan, J. A.; Fishman, M. C. *Nature* **1995**, *377*, 239−242.
(4) Fisslthaler, B.; Popp, R.; Kiss, L.; Potente, M.; Harder, D. R.; Fleming, I.; Busse, R. *Nature* **1999**, *401*, 493−497.
(5) Wei, X.-q.; Charles, I. G.; Smith, A.; Ure, J.; Feng, G.-j.; Huang, F.-p.; Xu, D.; Muller, W.; Moncada, S.; Liew, F. Y. *Nature* **1995**, *375*, 408−411.
(6) Ortiz de Montellano, P. R. *Cytochrome P-450: Structure, Mechanism, and Biochemistry*, 2nd ed.; Plenum Press: New York, 1995.
(7) Green, M. T.; Dawson, J. H.; Gray, H. B. *Science* **2004**, *304*, 1653−1656.
(8) Mayer, J. M. *Acc. Chem. Res.* **1998**, *31*, 441−450.
(9) Bordwell, F. G.; Cheng, J.-P.; Ji, G.-Z.; Satish, A. V.; Zhang, X. *J. Am. Chem. Soc.* **1991**, *113*, 9790−9795.
(10) Hoffman, B. M. *Proc. Natl. Acad. Sci. U.S.A.* **2003**, *100*, 3575−3578.
(11) Meunier, B.; de Visser, S. P.; Shaik, S. *Chem. Rev.* **2004**, *104*, 3947−3980.

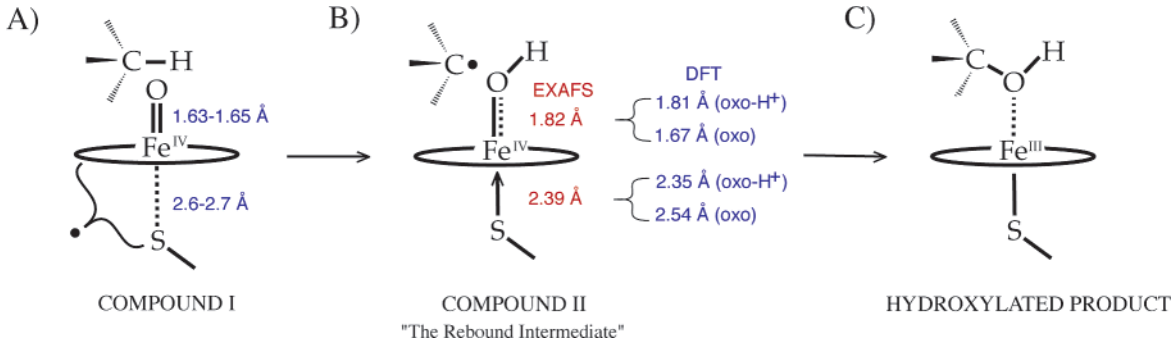

Figure 1. Rebound mechanism of cytochrome P450. (A) Compound I. Figure shows delocalization of the radical species over the porphyrin and thiolate ligands as well as the unusually long Fe−S bond predicted by density functional calculations. Distances given are from DFT. (B) The rebound intermediate. This figure illustrates that (except for the presence of the hydrocarbon radical) the P450 rebound intermediate and a thiolate-ligated compound II are equivalent. Distances in red are from XAS measurements on CPO-II. Those in blue are from DFT calculations on the protonated and unprotonated forms of a thiolate-ligated ferryl. (C) Weakly bound hydroxylated product.

X-ray absorption measurements generally suggest that these intermediates are Fe(IV)oxos. Fe−O distances of 1.67 and 1.69 Å have been found for CCP-I (pH 6) and Mb-II (pH not given).[16,17] Two independent studies of HRP-II (pH 6−7) have yielded oxo-like bonds of 1.64 and 1.70 Å,[7,18] but a bond of 1.93 Å (pH 7) has also been reported.[19] No EXAFS data have been published for CAT-II.

Fe−O stretching frequencies have also been reported for these intermediates. Resonance Raman measurements have provided values of 780 cm^{-1} (pD 4), 753 cm^{-1} (pH 4), 797 cm^{-1} (pH 8.5), and 775 cm^{-1} (pH 7) for HRP-II, CCP-I, Mb-II, and CAT-II, respectively.[20−23] The similarity between these stretching frequencies and the 790 cm^{-1} (pH 7) stretch found for the Fe(IV)oxo in both HRP-I and CPO-I suggests that these intermediates are authentic ferryl species.[18,24−27]

The origin of the ferryl bond length discrepancies is uncertain, but it is clear that X-ray crystallography generally yields longer ferryl bonds than EXAFS and Raman spectroscopies.[27,28] It is surprising that these longer bonds have been interpreted in terms of protonated ferryl species. High-valent ferryl species are generally thought to be electrophilic in nature.

(12) Berglund, G. I.; Carlsson, G. H.; Smith, A. T.; Szöke, H.; Henriksen, A.; Hajdu, J. *Nature* **2002**, *417*, 463−468.
(13) Hersleth, H.-P.; Dalhus, B.; Gørbitz, C. H.; Andersson, K. K. *J. Biol. Inorg. Chem.* **2002**, *7*, 299−304.
(14) Bonagura, C. A.; Bhaskar, B.; Shimizu, H.; Li, H.; Sundaramoorthy, M.; McRee, D. E.; Goodin, D. B.; Poulos, T. L. *Biochemistry* **2003**, *42*, 5600−5608.
(15) Murshudov, G. N.; Grebenko, A. I.; Brannigan, J. A.; Antson, A. A.; Barynin, V. V.; Dodson, G. G.; Dauter, Z.; Wilson, K. S.; Melik-Adamyan, W. R. *Acta Crystallogr.* **2002**, *D58*, 1972−1982.
(16) Chance, M.; Powers, L.; Poulos, T.; Chance, B. *Biochemistry* **1986**, *25*, 1266−1270.
(17) Chance, M.; Powers, L.; Kumar, C.; Chance, B. *Biochemistry* **1986**, *25*, 1259−1265.
(18) Penner-Hahn, J. E.; Eble, K. S.; McMurry, T. J.; Renner, M.; Balch, A. L.; Groves, J. T.; Dawson, J. H.; Hodgson, K. O. *J. Am. Chem. Soc.* **1986**, *108*, 7819−7825.
(19) Chance, B.; Powers, L.; Ching, Y.; Poulos, T.; Schonbaum, G. R.; Yamazaki, I.; Paul, K. G. *Arch. Biochem. Biophys.* **1984**, *235*, 596−611.
(20) Sitter, A. J.; Reczek, C. M.; Terner, J. *J. Biol. Chem.* **1985**, *260*, 7515−7522.
(21) Hashimoto, S.; Teraoka, J.; Inubushi, T.; Yonetani, T.; Kitagawa, T. *J. Biol. Chem.* **1986**, *261*, 11110−11118.
(22) Sitter, A. J.; Reczek, C. M.; Terner, J. *Biochim. Biophys. Acta* **1985**, *828*, 229−235.
(23) Chuang, W. J.; Heldt, J.; Van Wart, H. E. *J. Biol. Chem.* **1989**, *264*, 14209−14215.
(24) Kincaid, J. R.; Zheng, Y.; Al-Mustafa, J.; Czarnecki, K. *J. Biol. Chem.* **1996**, *271*, 28805−28811.
(25) Stone, K. L.; Behan, R. K.; Green, M. T. *Proc. Natl. Acad. Sci. U.S.A.* **2005**, *102*, 16563−16565.
(26) Egawa, T.; Proshlyakov, D. A.; Miki, H.; Makino, R.; Ogura, T.; Kitagawa, T.; Ishimura, Y. *J. Biol. Inorg. Chem.* **2001**, *6*, 46−54.
(27) Green, M. T. *J. Am. Chem. Soc.* **2006**, *128*, 1902−1906.
(28) Behan, R. K.; Green, M. T. *J. Inorg. Biochem.* **2006**, *100*, 448−459.

It is well-known that synchrotron radiation generates potent reducing equivalents in the form of solvated electrons.[12,14] The inability to quantitatively monitor changes in oxidation states during X-ray data collection is a general concern when working with high-valent species. Density functional calculations on heme model systems predict Fe(III)−OH bond lengths on the order of 1.81−1.85 Å.[27] Could the long Fe−O bonds of these "ferryl" complexes be indicative of ferric hydroxide species generated during data collection?

Given the important role that the ferryl pK_a may play in determining enzymatic function (eq 1), we have searched for an alternative method of determining the protonation states of ferryl species, one that does not suffer from the uncertainties associated with photoreduction. In what follows, we present evidence that Mössbauer spectroscopy can be used for this purpose.

Mössbauer spectroscopy is particularly suited for determining the composition and oxidation state of iron containing samples, but it has not generally allowed for structural characterization of iron centers. Recently, it was shown that density functional methods are capable of determining Mössbauer parameters with good accuracy. In general, quadrupole splittings, ΔE_Q, can be obtained to within 0.3 mm/s,[29] although errors on the order of 0.3−0.5 mm/s are not uncommon.[30] Isomer shifts, δ, are usually predicted to within 0.1 mm/s.[31] The accuracy with which these parameters can be determined suggests that theoretical methods can be used to obtain structural information from Mössbauer experiments. With this in mind, we examined CPO-II using a combination of density functional calculations and Mössbauer spectroscopy.

Computational Methods

All calculations were performed with Gaussian 03 using the B3LYP functional.[32] Geometry optimizations were performed with the 6-311G basis set. Quadrupole splittings, the asymmetry parameter, η, and ^{57}Fe hyperfine couplings were determined at the optimized geometries using the 6-311G basis set. Isomer shifts were determined at the optimized geometries using Neese's core properties (CP) basis set.[31] For this basis set, an integration grid containing 199 radial shells with 590 angular points per shell was used. The electron density at the Fe nucleus was determined using the Atoms In Molecules (AIM) option in Gaussian 03.

(29) Zhang, Y.; Mao, J.; Godbout, N.; Oldfield, E. *J. Am. Chem. Soc.* **2002**, *124*, 13921−13930.
(30) Neese, F. *Curr. Opin. Chem. Biol.* **2003**, *7*, 125−135.
(31) Neese, F. *Inorg. Chim. Acta* **2002**, *337*, 181−192.
(32) Frisch, M. J.; et al. *Gaussian 03*; Gaussian, Inc.: Wallingford, CT, 2004.

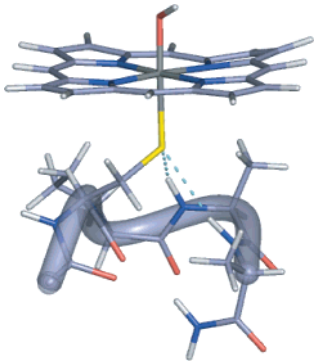

Figure 2. Large active-site model of the protonated form of chloroperoxidase compound II.

Calculations were performed on two types of model systems. The first was a porphine complex that on average contained 44 atoms. The second was a larger active-site model that was taken from a CPO crystal structure.[33] These larger calculations (88 atoms for CPO-II) differed from the smaller set in that a portion of the proximal helix was included and all atoms except for an inner core surrounding Fe (~30 atoms) were frozen during geometry optimizations. The inclusion of the proximal helix allowed for the consideration of important hydrogen-bonding between the helix and the axial-thiolate, while the geometry constraints allowed us to examine structures that more closely resembled those found in the enzyme. The large CPO model is shown in Figure 2. Initial geometries were obtained from a crystal structure of ferric CPO. The proximal helix was modeled with five residues (Cys29−Asn33). All residues except cysteine, proline, and glycine were converted into alanine, and the peptide chain was capped with hydrogens. During geometry optimizations, the positions of all atoms except Fe, the distal ligand, the porphyrin nitrogens, α-carbons, *meso*-carbons, *meso*-hydrogens, and a portion of the proximal ligand (SCH_2-CH) were constrained to their position in the ferric crystal structure.

Experimental Procedures

Purification of Chloroperoxidase. Chloroperoxidase was obtained from the filamentous fungus *Caldariomyces fumago* (ATCC 16373). *C. fumago* was grown in fructose salts media at 25 °C, according to established methods.[34] For ^{57}Fe cultures, $^{57}FeCl_3$ was added as the sole iron source. *C. fumago* secretes chloroperoxidase into the growth media. After 12 days, the media was collected, filtered, and subjected to two rounds of acetone precipitation. Cold acetone (−20 °C) was added to the media slowly with constant stirring to 35% (v/v). Gel precipitation occurred at −20 °C after an hour. Cold acetone (−20 °C) was added again for protein precipitation to 60% (v/v). Precipitation of CPO occurred overnight at −20 °C. Protein was centrifuged at 6000*g* for 5 min, and the solution was decanted. CPO was dissolved in 20 mM KPhos (pH 5.9), loaded onto a 100-mL SourceQ (Amersham Biosciences) column, and eluted with a linear gradient of 0−1 M NaCl. Fractions with an *Rz* (OD_{400nm}/OD_{280nm}) value of ≥1.4 were collected.

Preparation of $^{57}FeCl_3$. ^{57}Fe (Pennwood Chemicals) was added to a 20-mL vial that contained 10 mL of concentrated HCl and allowed to react at 80 °C until ^{57}Fe was visibly consumed. A typical culture contained 50 μM $^{57}FeCl_3$.

Freeze-Quenched Samples. A four-syringe ram freeze-quench apparatus from Update Instruments (Madison, WI) was used for all freeze-quench experiments. Reactants were mixed through an appropriate length aging line at room temperature and sprayed into cold isopentane, −140 °C. Samples were packed into a Mössbauer sample holder for analysis.

Preparation of CPO-II. ^{57}Fe (4mM) enriched chloroperoxidase and 37.5 mM reductant (ascorbic acid or *p*-phenolsulfonic acid) were reacted with 75 mM oxidant (peracetic acid or hydrogen peroxide) in the appropriate buffer. A 2:1 reaction of protein/reductant solution and oxidant was quenched in cold isopentane (−140 °C) 28 ms or 250 ms after mixing. Formation of CPO-II with *p*-phenolsulfonic acid as reductant was quenched 5 ms after mixing. All reactions were at room temperature.

Preparation of CPO-I for Cryoreduction. ^{57}Fe (4mM) enriched chloroperoxidase was reacted with 80 mM peracetic acid in 100 mM Kphos, pH 6.5, containing 15% (v/v) glycerol. A 2:1 reaction of protein and peracetic acid was quenched into cold isopentane (−140 °C) 10 ms after mixing.

Cryogenic Reduction of CPO-I and Annealing. Freeze-quenched 10-ms samples of CPO-I containing glycerol were irradiated at the γ-irradiation facility of the Breazeale nuclear reactor at Pennsylvania State University using a ^{60}Co source (35 krad/h); a total dose of 3.6 MRad was applied. Samples were maintained at 77 K during irradiation by immersion in liquid N_2. The cryoreduced samples were annealed by immersion in a dry ice and isopentane bath (−80 °C). All samples were analyzed by Mössbauer spectroscopy before and after cryoreduction and annealing experiments.

Mössbauer Spectroscopy. Mössbauer spectra were recorded on a spectrometer from WEB research (Edina, MN) operating in the constant acceleration mode in a transmission geometry. Spectra were recorded with the temperature of the sample maintained at 4.2 K. For low-field spectra, the sample was kept inside an SVT-400 dewar from Janis (Wilmington, MA), and a magnetic field of 40 mT was applied parallel to the γ-beam. For high-field spectra, the sample was kept inside a 12SVT dewar (Janis), which houses a superconducting magnet that allows for application of variable magnetic fields between 0 and 8 T parallel to the γ-beam. The quoted isomer shifts are relative to the centroid of the spectrum of a metallic foil of α-Fe at room temperature. Data analysis was performed using the program WMOSS from WEB research.

Results

Calculation of Mössbauer Parameters. Calculated Mössbauer parameters have not been previously reported for a protonated ferryl heme, and it was not known if ΔE_Q and δ were significantly affected by protonation. We first examined this possibility by calculating Mössbauer parameters for the ferryl forms of CPO-II. To calibrate our methods, we also examined different iron oxidation states, spin states, and axial ligations.

The results of our calculations are shown in Table 1 along with experimental results.[35−37] There it can be seen that the porphine model provides isomer shifts that are in good agreement with those obtained experimentally. The quadrupole splittings obtained with this model display the proper trends in sign and magnitude. Calculations on the larger active-site models yield similar isomer shifts, but the quadrupole splittings are greatly improved. For the ferric and ferrous forms of the enzyme, the agreement between theory and experiment is quite good. The improvement in predicted ΔE_Q most likely results from our geometry constraints. For each CPO model, 60 atoms were constrained to their positions in the ferric crystal structure. Only an inner core surrounding Fe was allowed to move (~30 atoms).

(33) Sundaramoorthy, M.; Terner, J.; Poulos, T. L. *Structure* **1995**, *3*, 1367−1377.
(34) Pickard, M. A. *Can. J. Microbiol.* **1981**, *27*, 1298−1305.
(35) Champion, P. M.; Chiang, R.; Münck, E.; Debrunner, P.; Hager, L. P. *Biochemistry* **1975**, *14*, 4159−4166.
(36) Champion, P. M.; Münck, E.; Debrunner, P. G.; Hollenberg, P. F.; Hager, L. P. *Biochemistry* **1973**, *12*, 426−435.
(37) Sharrock, M.; Debrunner, P. G.; Schulz, C.; Lipscomb, J. D.; Marshall, V.; Gunsalus, I. C. *Biochim. Biophys. Acta* **1976**, *420*, 8−26.

Table 1. Mössbauer Parameters for Chloroperoxidase[a]

distal ligand	oxidation state	spin state	optimized porphine (mm/s)		constrained optimization (mm/s)		experiment (mm/s)		ref
			δ	ΔE_Q	δ	ΔE_Q	δ	ΔE_Q	
none	II	2	0.68	−1.85	0.67	−2.56	0.86	−2.50	35
CO	II	0	0.31	0.22	0.30	0.59	0.29	0.52	36
water	III	1/2	0.38	−2.66	0.38	−3.28	0.30	−3.01	36
none[b]	III	5/2	0.43	0.60	0.39	0.75	0.44	0.79	37
oxo-H	IV	1	0.08	1.84	0.10	2.06	0.10 ± 0.03	2.06 ± 0.03	this work
oxo^-	IV	1	0.13	0.63	0.12	1.00	0.11 ± 0.03	1.59 ± 0.05	this work

[a] Constrained optimizations used the ferric crystal structure as starting point. These calculations differed from the smaller (porphine only) set in that a portion of the proximal helix was included and all atoms except for an inner core surrounding Fe (~30 atoms) were frozen during geometry optimizations. [b] Experimental parameters for the high-spin ferric form of CPO are not available. Values shown are from measurements on cytochrome P450.

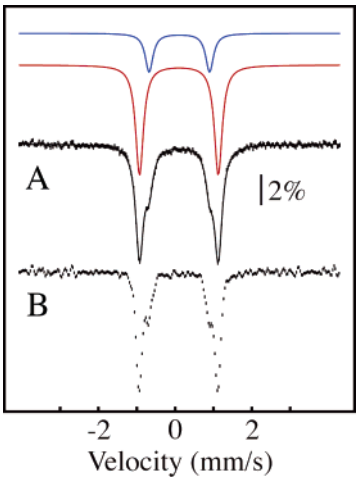

Figure 3. Mössbauer spectrum of CPO-II pH 6.5, 250-ms quench time. Similar results were obtained with a 28-ms quench. Spectrum A shows raw data; solid line is best fit to two quadrupole doublets ($\delta = 0.10$ mm/s, $\Delta E_Q = 2.06$ mm/s) and ($\delta = 0.11$ mm/s, $\Delta E_Q = 1.59$ mm/s). Spectrum B was obtained from a Fourier transform analysis of the data, which removes the line width of the ^{57}Co(Rh) source and highlights the presence of two distinct species.

Presumably, these constraints allow us to examine structures that more closely resemble those found in the enzyme. Application of the same methods to the ferryl intermediates suggests that ΔE_Q is significantly affected by protonation. These computations led us to perform the first Mössbauer experiments on CPO-II.

Mössbauer Spectroscopy. Seven CPO-II samples were prepared by mixing ferric CPO with peracetic acid and ascorbate (Experimental Procedures). The 4.2-K/40-mT spectrum of a representative sample is shown in Figure 3A. This spectrum exhibits two asymmetric peaks at approximately −0.9 mm/s and +1.1 mm/s.[38] The inner shoulders of these peaks suggest the presence of a pair of symmetric quadrupole doublets with similar isomer shifts. To enhance the resolution of the spectrum, we removed the line width of the ^{57}Co(Rh) source (Figure 3B), using a Fourier transform technique.[39] The presence of two distinct quadrupole doublets is clearly evident.

Initial fits of the raw data were performed with the widths of all four lines constrained to be equal (solid line, Figure 3A).

Table 2. Mössbauer Parameters of Ferryl Heme Complexes

system	trans ligand	oxidation/spin state	(mm/s) δ	(mm/s) ΔE_Q	ref
JRP-I	histidine	IV ($S = 1$)	0.10	1.33	40
JRP-II	histidine	IV ($S = 1$)	0.03	1.59	41
CCP-I	histidine	IV ($S = 1$)	0.05	1.55	42
HRP-I	histidine	IV ($S = 1$)	0.08	1.25	43, 47
HRP-II	histidine	IV ($S = 1$)	0.03	1.61	47
CPO-I	cysteine	IV ($S = 1$)	0.14	1.02	44
Mb-II	histidine	IV ($S = 1$)	0.09	1.44	41
FeOTPP	1-mIm	IV ($S = 1$)	0.11	1.26	47
FeOTPP	pyridine	IV ($S = 1$)	0.10	1.56	47
FeOTMP	chloride	IV ($S = 1$)	0.07	1.35	45
$FeO(TMP\text{-}Br_4)^{\bullet+}$	methanol	IV ($S = 1$)	0.02	1.28	46
$FeO(TMP\text{-}Cl_8)^{\bullet+}$	methanol	IV ($S = 1$)	0.08	1.43	46
			0.08	1.39	avg
			0.04	0.17	RMSD

The parameters of the major component, isomer shift $\delta = 0.10 \pm 0.03$ mm/s and quadrupole splitting $\Delta E_Q = 2.06 \pm 0.03$ mm/s, are identical to the values calculated for a protonated ferryl species. The minor component has the following parameters: $\delta = 0.11 \pm 0.03$ mm/s and $\Delta E_Q = 1.59 \pm 0.05$ mm/s. The quadrupole splitting of the minority species is in reasonable agreement with the value predicted for an Fe(IV)oxo (Table 1) and in good agreement with the quadrupole splittings obtained for ferryl heme species (Table 2).[40−47]

Fits using two symmetric quadrupole doublets with equal line widths yield 74 ± 4% (mean and two standard deviations of the seven fits) of the major component and 26 ± 4% of the minor component. If we allow the line widths of the two species to differ by no more than 15%, we find the width of the minor component to be slightly (~10%) larger, resulting in 68 ± 7% of the major and 32 ± 7% of the minor ferryl species. Importantly, all fits yield nearly identical Mössbauer parameters.

To further characterize the two species of CPO-II, we recorded spectra in parallel magnetic fields of 4 and 7 T (Figure 4). The solid lines overlaid with the experimental data (hash

(38) Some CPO-II samples were found to contain a minor amount (<15%) of ferric CPO (see Figure 6, spectrum A1). Its relative amount can be estimated accurately from the prominent peak at +4 mm/s, which is well separated from the quadrupole doublets of CPO-II. We have removed the ferric contribution to the raw data prior to anaylsis of the spectral features of CPO-II.

(39) Dibar-Ure, C.; Flinn, P. A. *Mössbauer Effect Methodology*; Gruverman, I. J., Ed.; Plenum Press: New York, 1971; pp 245−262.

(40) Maeda, Y.; Higashimura, T.; Morita, Y. *Biochem. Biophys. Res. Commun.* **1967**, *29*, 362−367.
(41) Harami, T.; Maeda, Y.; Morita, Y.; Trautwein, A. X.; Gonser, U. *J. Chem. Phys.* **1977**, *67*, 1164−1169.
(42) Lang, G.; Spartalian, K.; Yonetani, T. *Biochim. Biophys. Acta* **1976**, *451*, 250−258.
(43) Schulz, C.; Chiang, R.; Debrunner, P. G. *J. Phys.* **1979**, *40*, C2-534.
(44) Rutter, R.; Hager, L. P.; Dhonau, H.; Hendrich, M.; Valentine, M.; Debrunner, P. G. *Biochemistry* **1984**, *23*, 6809−6816.
(45) Wolter, T.; Meyer-Klaucke, W.; Müther, M.; Mandon, D.; Winkler, H.; Trautwein, A. X.; Weiss, R. *J. Inorg. Biochem.* **2000**, *78*, 117−122.
(46) Weiss, R.; Mandon, D.; Wolter, T.; Trautwein, A. X.; Müther, M.; Bill, E.; Gold, A.; Jayaraj, K.; Terner, J. *J. Biol. Inorg. Chem.* **1996**, *1*, 377−383.
(47) Schulz, C. E.; Rutter, R.; Sage, J. T.; Debrunner, P. G.; Hager, L. P. *Biochemistry* **1984**, *23*, 4743−4754.

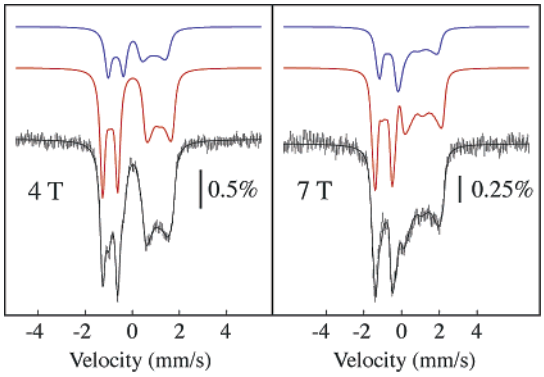

Figure 4. Mössbauer spectra (hash marks) of CPO-II pH 6.5, 28-ms quench time, recorded at 4.2 K in externally applied magnetic fields of 4 and 7 T oriented parallel to the γ-beam. The solid lines are simulations assuming the slow relaxation limit and using the following parameters: $S = 1$, $D = +23$ cm^{-1}, $E/D = 0.0$, $\mathbf{g} = (2.1, 2.1, 2.0)$, $\eta = 0$, and $\mathbf{A}/g_N\beta_N = (-20, -20, -7)$ T for both species and using the Mössbauer parameters (δ and ΔE_Q) listed in Table 1. The red (blue) line above the data is the individual contribution of the major (minor) component.

marks) were calculated using an $S = 1$ spin Hamiltonian. Since the experimental data do not allow for the unique determination of the spin Hamiltonian parameters, both species were assumed to have the following parameters, which are typical of ferryl heme species: zero-field splitting parameters $D = +23$ cm^{-1} and $E/D = 0$, $\mathbf{g} = (2.1, 2.1, 2.0)$, asymmetry parameter $\eta = 0$, $\mathbf{A}/g_N\beta_N = (-20, -20, -7)$ T.[48,49] Mössbauer parameters (δ and ΔE_Q) were taken from the 40 mT data. The individual contribution of the major (minor) component to the spectrum is shown as a red (blue) line above the data. The high-field spectra reveal that D and ΔE_Q are positive for both intermediates. The data shown in Figure 4 are fully consistent with both species having an $S = 1$ ground state.

Cryogenic Reduction Experiments. To gain further insight into the ferryl species of CPO-II, we turned to cryogenic reduction experiments. In these experiments, metalloenzyme−glycerol mixtures are exposed to γ-irradiation at low temperatures (normally 77 K). This generally allows for reduction of the metal center without subsequent chemistry.[50] Annealing at elevated temperatures results in relaxation of the cryoreduced species and, perhaps, the observation of reactive intermediates that follow reduction in the catalytic cycle.

In our experiments, samples containing chloroperoxidase compound I (CPO-I) and glycerol were exposed to γ-irradiation at 77 K. Our goal was to prepare CPO-II exclusively in its unprotonated form through the cryoreduction of CPO-I, an authentic Fe(IV)oxo species.[25,26,51] The hope was that this unprotonated form of CPO-II would be stable at 77 K, and that proton transfer to the ferryl oxygen could be observed upon annealing at higher temperatures (Figure 5).

The results of these experiments are illustrated in Figure 6. Panel C shows the cryoreduction of CPO-I (CR-CPO-I) and panel D shows the annealing of cryoreduced CPO-I. Since (1) samples of CPO-I contain minor amounts of ferric CPO and (2) the yield of CR-CPO-I is less than 100%, it was necessary

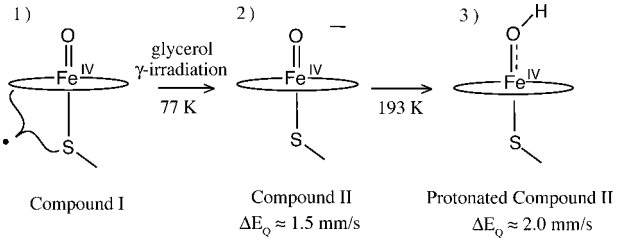

Figure 5. Cryoreduction and annealing. Sample containing CPO-I and glycerol is prepared. γ-Irradiation at 77 K generates free electrons which reduce CPO-I forming unprotonated CPO-II. This species is annealed at 193 K to allow for proton delivery.

to perform control experiments that examined (1) the cryoreduction of ferric CPO (panel A) and (2) the annealing of noncryoreduced CPO-I (panel B).

Panel A reveals the effect of cryoreduction on the ferric enzyme. A1 is the spectrum of ferric CPO. This spectrum can be simulated using a spin Hamiltonian formalism in the slow relaxation limit with the following parameters: $S = 1/2$, $\mathbf{g} = (1.84, 2.26, 2.63)$, $\delta = 0.30$ mm/s, $\Delta E_Q = 2.90$ mm/s, $\eta = -2$, and $\mathbf{A}/g_N\beta_N = (-46.0, +7.9, +28.4)$ T. These parameters are very similar to those reported previously.[36] A2 shows the spectrum of the ferric sample after cryoreduction. The amount of ferric CPO is markedly reduced, and several new features are present, of which two sharp lines at −0.4 mm/s and +2.1 mm/s are most prominent. Deconvolution of spectrum A2 reveals that the sample contains 51% ferric CPO (shown as a solid line overlaid with the experimental data in A2). Removal of the ferric contribution yields **A3**, the reference spectrum for the ferrous species formed during cryoreduction. The majority of the intensity in A3 emanates from a quadrupole doublet with $\delta = 0.85$ mm/s and $\Delta E_Q = 2.49$ mm/s. This species, which accounts for 45% of the total Fe and 92% of the cryoreduced products in the sample, has parameters that are typical of high-spin ferrous heme proteins.[35] In addition to this major component, there are also three minor peaks detectable in A3. The identities of these features are presently not well understood.

Panel B shows the effect of annealing on CPO-I (note this sample is *not* cryoreduced). Shown in B1 is the spectrum of CPO-I. Deconvolution of this spectrum shows that the sample contains 90% CPO-I and 10% ferric CPO. The spectrum of ferric CPO is shown as a solid black line. The spectrum of CPO-I can be simulated (solid red line) using a spin Hamiltonian formalism in the slow relaxation limit with parameters nearly identical to those previously published:[44] $S_{eff} = {}^1/_2$, $\mathbf{g} = (2.0, 2.0, 2.0)$, $\delta = 0.15$ mm/s, $\Delta E_Q = 1.02$ mm/s, $\eta = 0$, and $\mathbf{A}/g_N b_N = (-30.5, -30.5, -6.0)$ T. Shown in B2 is the Mössbauer spectrum of the CPO-I sample after annealing at −80 °C for 30 min. The sample's spectrum changes significantly. The amount of ferric CPO in the sample increases from 10 to 74%, as depicted by the solid line plotted in B2, demonstrating that CPO-I decays at −80 °C to ferric CPO. This conversion is shown in the difference spectrum B3 (B2−B1). The features pointing up in this spectrum correspond to the species that decays at −80 °C, while the features pointing down originate from the species generated during this process. The solid line was obtained, by adding equal amounts of the spectra of CPO-I (pointing upward) and ferric CPO (pointing downward). The agreement between this line and the experimental difference spectrum indicates that CPO-I converts to ferric CPO upon annealing at −80 °C.

(48) Debrunner, P. G. *Phys. Bioinorg. Chem. Ser.* **1989**, *4*, 137−234.
(49) Oosterhuis, W. T.; Lang, G. *J. Chem. Phys.* **1973**, *58*, 4757−4765.
(50) Davydov, R.; Kuprin, S.; Gräslund, A.; Ehrenberg, A. *J. Am. Chem. Soc.* **1994**, *116*, 11120−11128.
(51) CPO-I is known to have a ferryl stretching frequency of 790 cm^{-1}. Egawa, T.; Proshlyakov, D. A.; Miki, H.; Makino, R.; Ogura, T.; Kitagawa, T.; Ishimura, Y. *J. Biol. Inorg. Chem.* **2001**, *6*, 46−54.

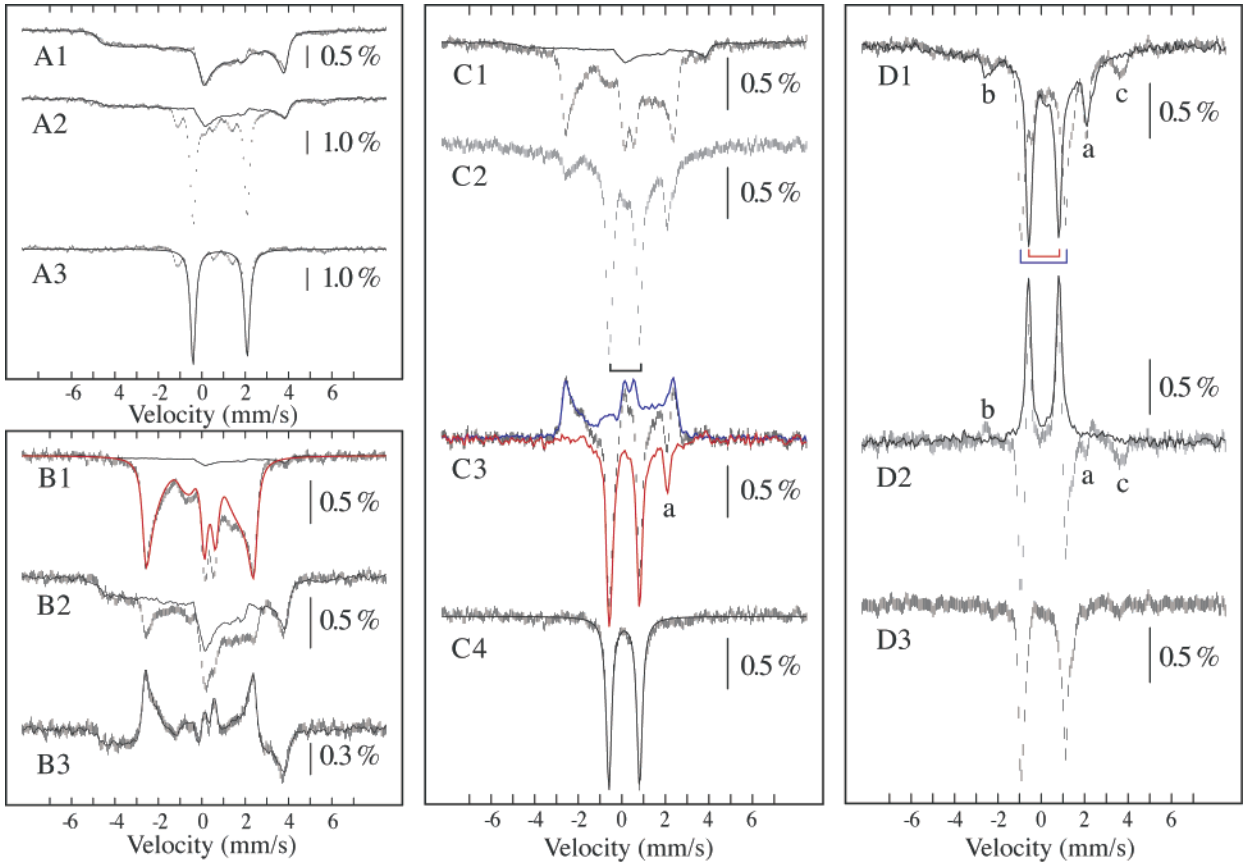

Figure 6. Cryogenic reduction and annealing experiments. (A) Cryoreduction of ferric CPO. (B) Annealing of CPO-I (not cryoreduced). (C) Cryoreduction of CPO-I. (D) Annealing of cryoreduced CPO-I. See text for discussion.

Panel C shows the effect of cryoreduction on CPO-I. C1 is the spectrum recorded before cryoreduction. The sample contains 22% ferric CPO (solid line) and 78% CPO-I. Cryoreduction results in the spectrum shown in C2. There is a decrease in the features of CPO-I and the generation of two intense lines at −0.58 mm/s and +0.80 mm/s, as indicated by the bracket. C3 shows the difference spectrum (C2 − C1). The features pointing up represent the fraction of the sample that is reduced during cryoreduction. Adding back 53% of CPO-I (C3, blue solid line) to the difference spectrum (C3, hash marks) results in the solid red line in C3. In addition to the pair of intense lines, a new line, which is labeled "a", appears. The position of this line is identical to that of the high-energy line of CR-ferric-CPO (compare the line at 2.1 mm/s in spectrum A3 to line "a"). After adding and removing the appropriate contributions of ferric CPO (10%) and CR-ferric-CPO (13%), we obtain spectrum C4, which is a reference spectrum for CR-CPO-I. It can be simulated with one sharp quadrupole doublet having the following paramters: $\delta = 0.12$ mm/s and $\Delta E_Q = 1.41$ mm/s. These parameters, which are typical of ferryl heme species, are similar (but not identical) to the parameters of the minor component ($\delta = 0.11$ mm/s, $\Delta E_Q = 1.59$ mm/s) observed in our freeze-quenched CPO-II samples. We attribute the 0.2 mm/s difference in quadrupole splitting to the inability of the cryoreduced intermediate to relax its structure at 77 K.

Panel D reveals the effect of annealing the CR-CPO-I sample at −80 °C for 30 min. D1 shows the spectrum of CR-CPO-I before (solid line) and after (hash marks) annealing. Several changes are observed. The amount of CPO-I decreases upon annealing (peak "b"), and the quadrupole doublet of the ferryl species generated by cryoreduction (red bracket) decreases in intensity. Two major species are formed upon annealing: The intensity of ferric CPO increases (peak "c"), and a new quadrupole doublet, indicated by the blue bracket, appears. Since CPO-I decays preferentially to ferric CPO (panel B), the new quadrupole doublet must originate from the ferryl species generated during the cryoreduction of CPO-I. The difference spectrum shown in D2 illustrates this. Pointing up is the quadrupole doublet associated with CR-CPO-I. Upon annealing, this species is converted to the downward pointing quadrupole doublet features in D2. The reference spectrum of annealed CR-CPO-I (D3) was generated by removing the appropriate amounts of the other components from the raw data (hash marks in D1): 33% ferric CPO, 4% CPO-I, and 18% CR-ferric-CPO. To enhance the resolution of the quadrupole doublet features, we generated a reference spectrum for CR-CPO-I from spectra collected over a narrower range of Doppler velocities using the same approach (Figure 7A). It reveals the presence of three distinct quadrupole doublets. One component with $\delta = 0.29$ mm/s and $\Delta E_Q = 2.30$ mm/s makes up 6% of the total sample (solid line, Figure 7A). The identity of this minor species is unknown. Removing its contribution from the spectrum in Figure 7A results in the hash marked spectrum shown in Figure 7B. This spectrum can be simulated using two quadrupole doublets with parameters that are essentially identical to those obtained for freeze-quenched CPO-II. These species account for 29% ($\delta = 0.10$ mm/s, $\Delta E_Q = 2.08$ mm/s) and 10% ($\delta = 0.11$ mm/s, $\Delta E_Q = 1.60$ mm/s) of the total area, giving an ∼74:26 ratio of the two components. Given the experimental error,

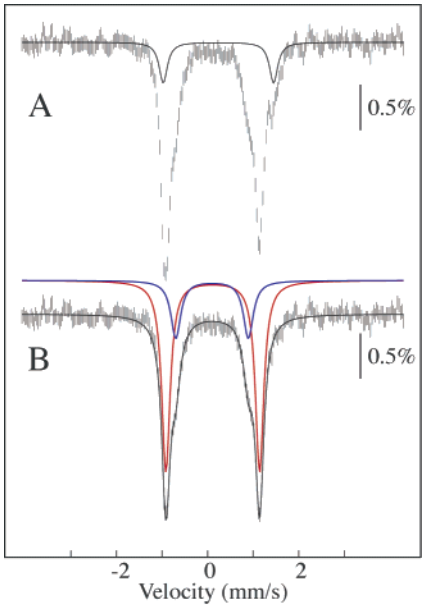

Figure 7. (A) Reference spectrum for the species generated during the annealing process. This spectrum is similar to D3, but it was generated from spectra collected over a narrower range of Doppler velocities. The solid line shows the quadrupole doublet (6% of the total intensity, δ = 0.29 mm/s, ΔE_Q = 2.30 mm/s) of an unidentified species. (B) Reference spectrum obtained by removing contributions from the unidentified species (solid line in A). The quadrupole doublets shown in (B) represent 29% (δ = 0.10 mm/s, ΔE_Q = 2.08 mm/s) and 10% (δ = 0.11 mm/s, ΔE_Q = 1.60 mm/s) of the total intensity.

this ratio is indistinguishable from the values obtained in our freeze-quench experiments.

Preparation of CPO-II under Different Conditions. To aid in the identification of the two intermediates, we attempted to change their relative concentrations by varying the pH. Surprisingly, however, we find that the ratio of the intermediates is independent of pH. From pH 4.5 to 6.9, we obtain the same ~70:30 ratio (Figure S.1, Supporting Information). We have also prepared CPO-II with different oxidants and reductants. Hydrogen peroxide/ascorbic acid and peracetic acid/*p*-phenolsulfonic acid preparations of CPO-II contain the ferryl intermediates in the same ~70:30 ratio (Figures S.2 and S.3, Supporting Information).

Discussion

Three results strongly suggest that the CPO-II majority species (ΔE_Q = 2.06 mm/s) is an Fe(IV)OH intermediate. These are (1) the 1.82 Å Fe−O bond length obtained from EXAFS measurements, (2) the excellent agreement between calculated and measured Mössbauer parameters, and (3) the cryogenic reduction and annealing of CPO-I. Our experiments indicate the minority species is an Fe(IV) intermediate as well. The Mössbauer parameters of the minor component are typical of six-coordinate ferryl heme species (Table 2), and they are similar to the values obtained for the Fe(IV)oxo of CR-CPO-I. These results have led us to assign the major and minor components as the protonated and unprotonated forms of CPO-II. At odds with this assignment, however, is the pH invariance of the relative concentrations of the major and minor components.

The insensitivity of the relative concentrations to pH is puzzling. This result, by itself, suggests that the intermediates are not related by a protonation event, and from it one might conclude that the major and minor components are (1) the protonated form of CPO-II and (2) some unidentified (nonferryl) Fe(IV) species. However, the reaction in question must be considered. CPO-I (an authentic Fe(IV)oxo radical species) is generated by the two-electron oxidation of ferric CPO. This oxidation is performed with an oxygen transfer reagent (H_2O_2 or PA). Once CPO-I is formed, two one-electron reductions and two protonations are required to convert the oxo ligand to water and return the enzyme to its ferric state. The only Fe(IV) species one would expect to be generated during this process are the Fe(IV)O and Fe(IV)OH intermediates.

It is important to note that the invariant ratio is not an artifact of sample preparation or protein/reagent impurities: we can generate CPO-I in excess of 90%, the enzyme returns quantitatively to the ferric state with or without exogenous reductant, and we have obtained the same ratio of intermediate concentrations with different oxidants and reductants (Supporting Information). We also point out that the invariant ratio of component concentrations is in agreement with CPO-II's visible absorption spectrum, which shows no change over the enzyme's range of pH stability (pH 3−7).

Conclusion

Taken together, the results of our calculations and Mössbauer experiments suggest that CPO-II is ~70% protonated. These results are in agreement with EXAFS experiments that put the Fe−O bond in CPO-II at 1.82 Å.[7] The Mössbauer parameters of the minority (30%) species are indicative of an Fe(IV)oxo intermediate, and we assign it as such. The pH invariance of the 70:30 ratio, however, makes this assignment tentative.

Calculations on imidazole-ligated hemes suggest that an even larger change (ca. 1.4 mm/s) in quadrupole splitting occurs upon ferryl protonation in these systems. Histidine-ligated Fe(IV)-OH porphyrin species are predicted to have $\Delta E_Q \approx$ 2.8 mm/s.[28] Mössbauer measurements at pH 7 have provided quadrupole splittings of 1.61, 1.44, and 1.55 mm/s for HRP-II, Mb-II, and CCP-I, respectively,[42,43,47] indicating that these intermediates are not protonated. In contrast, Mössbauer measurements on a ferryl form of cytochrome P450 (pH 7) have provided a quadrupole splitting of 1.94 mm/s,[52] which is in good agreement with ΔE_Q = 2.06 mm/s obtained for the major component of CPO-II. Taken together, these results suggest thiolate ligation (or axial coordination by a strongly donating anionic ligand) may be a prerequisite for the generation of basic ferryls in heme enzymes.

Acknowledgment. This research was supported by the National Science Foundation (M.T.G.), the Petroleum Research Fund (M.T.G.), and the Arnold and Mabel Beckman Foundation (M.T.G.). R.K.B. is supported by a grant from the Herman Frasch Foundation. We thank Candace C. Davison from the Breazeale Nucelar Reactor Facility, Penn State University, for her assistance with the low-temperature γ-irradiation experiments.

Supporting Information Available: Complete author list for ref 32. Mössbauer spectra. This material is available free of charge via the Internet at http://pubs.acs.org.

JA057876W

(52) Schünemann, V.; Jung, C.; Terner, J.; Trautwein, A. X.; Weiss, R. *J. Inorg. Biochem.* **2002**, *91*, 586−596.